JOURNAL OF GEOPHYSICAL RESEARCH, VOL. 112, B07310, doi:10.1029/2005JB003772, 2007

The instantaneous rate dependence in low temperature laboratory rock friction and rock deformation experiments

N. M. Beeler,[1] T. E. Tullis,[2] A. K. Kronenberg,[3] and L. A. Reinen[4]

Received 11 April 2005; revised 6 December 2006; accepted 9 March 2007; published 12 July 2007.

[1] Earthquake occurrence probabilities that account for stress transfer and time-dependent failure depend on the product of the effective normal stress and a lab-derived dimensionless coefficient a. This coefficient describes the instantaneous dependence of fault strength on deformation rate, and determines the duration of precursory slip. Although an instantaneous rate dependence is observed for fracture, friction, crack growth, and low temperature plasticity in laboratory experiments, the physical origin of this effect during earthquake faulting is obscure. We examine this rate dependence in laboratory experiments on different rock types using a normalization scheme modified from one proposed by Tullis and Weeks [1987]. We compare the instantaneous rate dependence in rock friction with rate dependence measurements from higher temperature dislocation glide experiments. The same normalization scheme is used to compare rate dependence in friction to rock fracture and to low-temperature crack growth tests. For particular weak phyllosilicate minerals, the instantaneous friction rate dependence is consistent with dislocation glide. In intact rock failure tests, for each rock type considered, the instantaneous rate dependence is the same size as for friction, suggesting a common physical origin. During subcritical crack growth in strong quartzofeldspathic and carbonate rock where glide is not possible, the instantaneous rate dependence measured during failure or creep tests at high stress has long been thought to be due to crack growth; however, direct comparison between crack growth and friction tests shows poor agreement. The crack growth rate dependence appears to be higher than the rate dependence of friction and fracture by a factor of two to three for all rock types considered.

Citation: Beeler, N. M., T. E. Tullis, A. K. Kronenberg, and L. A. Reinen (2007), The instantaneous rate dependence in low temperature laboratory rock friction and rock deformation experiments, *J. Geophys. Res.*, *112*, B07310, doi:10.1029/2005JB003772.

1. Introduction

[2] Stress changes alter earthquake recurrence probabilities [e.g., *Stein et al.*, 1997] depending on the type of stress change, the characteristics of the unperturbed probability distribution, and the dependence of fault failure time on stress. To illustrate, consider an idealized case: the effect of a static stress change on the probability density of earthquake recurrence of an event with a known, log normal distribution of recurrence intervals [e.g., *Stein et al.*, 1997] (Figure 1, black)

$$P(t_r) = \frac{1}{s t_r \sqrt{2\pi}} \exp\left(-\left[\ln t_r - \bar{l}_{t_r}\right]^2 \Big/ 2s^2 \right), \qquad (1)$$

where t_r is recurrence interval, $\bar{l}_{t_r}$ is the average log recurrence interval and s is the standard deviation of log recurrence interval (Figure 1, black). The tectonic stressing rate $\dot{\tau}$ is constant. We consider the importance of the assumed fault strength by using two different laboratory-based failure criteria. Given a stress threshold failure relation and an increase in shear stress $\Delta\tau$ applied at time $t_r = t_0$, the times for potential recurrences with $t_r > t_0 + \Delta\tau/\dot{\tau}\sigma$ are shortened by $\Delta\tau/\dot{\tau}$. Potential recurrences in the range $t_0 < t_r < t_0 + \Delta\tau/\dot{\tau}$ collapse onto $t_r = t_0$, and we have a density

$$\begin{aligned}
P &= \frac{1}{s t_r \sqrt{2\pi}} \exp\left(-\left[\ln t_r - \bar{l}_{t_r}\right]^2 \Big/ 2s^2 \right) && 0 < t_r < t_0 \\
P &= \frac{1}{s t_r \sqrt{2\pi}} \exp\left(-\left[\ln t_r - \bar{l}_{t_r}\right]^2 \Big/ 2s^2 \right) \\
&\quad + \int_{t_0}^{t_0+\Delta\tau/\dot{\tau}} \frac{1}{s t_r \sqrt{2\pi}} \exp\left(-\left[\ln t_r - \bar{l}_{t_r}\right]^2 / 2s^2 \right) dt_r && t_r = t_0 \\
P &= \frac{1}{s t_r \sqrt{2\pi}} \exp\left(-\left[\ln\left(t_r + \frac{\Delta\tau}{\dot{\tau}} \right) - \bar{l}_{t_r} \right]^2 \Big/ 2s^2 \right) && t_r > t_0
\end{aligned} \qquad (2)$$

Thus at the moment of the stress change, the instantaneous expected rate of earthquake recurrence is transiently high

[1] US Geological Survey, Menlo Park, California, USA.
[2] Brown University, Providence, Rhode Island, USA.
[3] Texas A&M University, College Station, Texas, USA.
[4] Pomona College, Pomona, California, USA.

0148-0227/07/2005JB003772$09.00

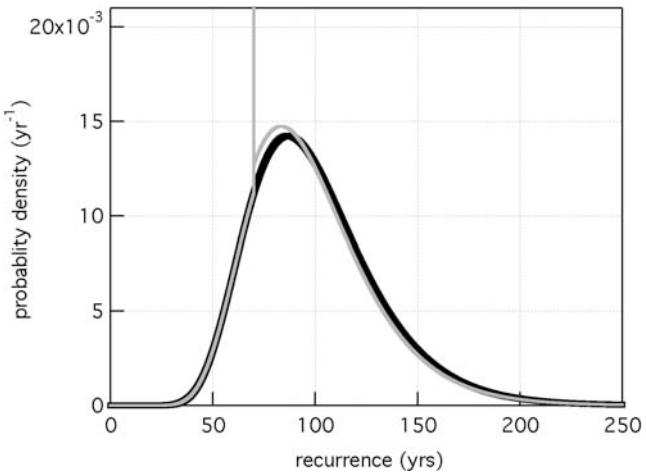

Figure 1. Log normal distribution of recurrence intervals for $\bar{l}_{t_r}$ = 4.6 ln(yr), s = 0.31 ln(yr) (black). Also shown is the probability density for recurrence of a threshold failure model, subject to a stress increase $\Delta\tau$ = 0.3 MPa at t = 70 yr (grey).

(Figure 1, grey), depending on the size of the stress change ($\Delta\tau$), the stressing rate ($\dot{\tau}$), and on when the stress change occurs (t_0).

[3] Using a threshold failure relationship, all of the time dependence of earthquake probability arises from the nature of the stress change and the assumed form of the probability density distribution while the fault failure criteria, having no time dependence, does not contribute. In contrast to threshold failure, laboratory observations of intact rock failure and stick-slip sliding on preexisting faults invariably show second order dependencies on time of one sort or another, principally static fatigue where time of failure depends on the size of the stress change and initial temporal proximity to failure [e.g., *Scholz*, 1972; *Kranz*, 1980]. Other time-dependent phenomenon include delayed failure and precursory slip, most obvious in stick-slip sliding tests [e.g., *Dieterich*, 1992]. These are believed to arise from the same kind of underlying physical mechanism as is responsible for static fatigue, resulting in a small positive, nonlinear dependence of fault strength on sliding rate.

[4] When the failure criteria is time-dependent, the recurrence probabilities are quite different from the threshold model prediction. For laboratory observations, a stress change alters the failure time by some amount, which typically depends on how close the fault was to failure prior to the stress change [e.g., *Scholz*, 1972; *Dieterich*, 1994]. This fundamental time dependence of rock fracture and stick-slip failure stress can be described empirically using a relation proposed by *Dieterich* [1992; 1994]:

$$\frac{\tau}{\sigma_e} = \mu_* + a \ln \frac{V}{V_*} - b \frac{\delta}{d_c} \tag{3}$$

where δ is slip, σ_e is the effective normal stress, τ is shear stress in the direction of slip, and V is slip rate. a and b are experimentally determined and are second order relative to the nominal friction $\mu*$ and $V*$ is the slip velocity when $\mu* = 0$ and δ = 0. d_c is a characteristic slip distance. This is a failure relation used in probability calculations by *Stein et al.* [1997] and subsequent others and in seismicity rate estimates by *Dieterich* [1994] and *Gomberg et al.* [2000]. In our recurrence example this relation produces a recurrence probability density due to static stress change of the form

$$P(t) = \frac{1}{st\sqrt{2\pi}} \exp\left(-\left[\ln(t) - \bar{l}_{t_r}\right]^2 / 2s^2\right) \qquad t < t_0$$

$$P(t) = \frac{\frac{1}{s(t+t_c)\sqrt{2\pi}} \exp\left(-\left[\ln(t+t_c) - \bar{l}_{t_r}\right]^2 / 2s^2\right)}{1 + \left[\exp(-\Delta\tau / a\sigma_e) - 1\right] \exp\left[-\dot{\tau}(t - t_0)/a\sigma_n\right]} \qquad t \geq t_0 \tag{4}$$

(Figures 2a–2b). A derivation of equation (4) is included in the Appendix. The result is a transient increase of different amplitude than obtained for the threshold example (Figure 1), and it is spread out over a longer time interval. During the years immediately after the stress transfer event, the recurrence probability density is dramatically enhanced over the unperturbed probability density and over the threshold model (Figure 1). How much the probability density is

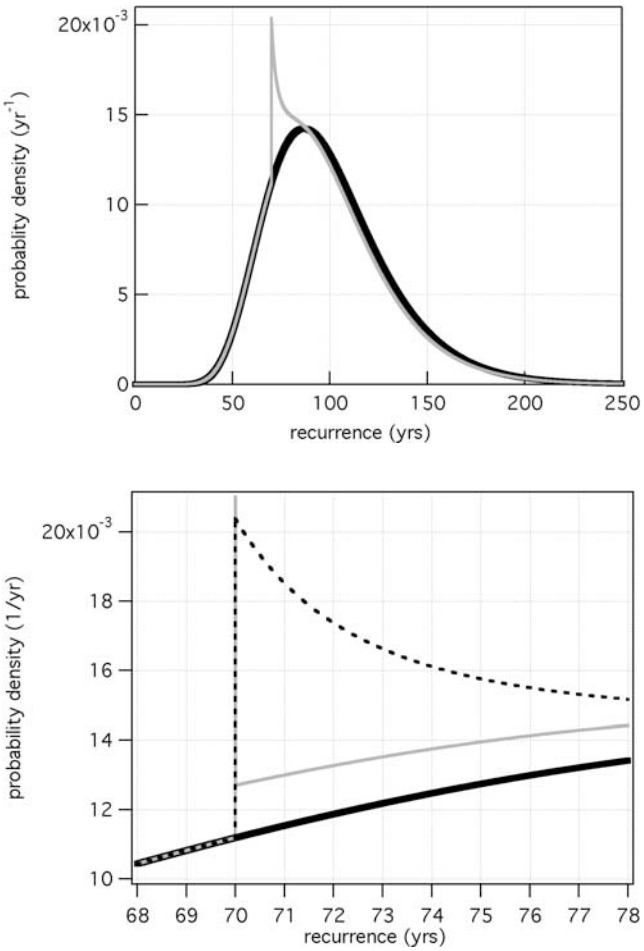

Figure 2. (a) Log normal distribution of recurrence intervals with $\bar{l}_{t_r}$ = 4.6 ln(yr), s = 0.31 ln(yr) (black). Also shown is the probability density for recurrence of a simple failure model [*Dieterich*, 1994] subject to a stress increase $\Delta\tau$ = 0.3 MPa, at t = 70 yr, with $\dot{\tau}$ = 10MPa/100 yr, a = 0.005, b = 0.01, σ_e = 100 MPa, d_c = 5 μm (grey). (b) Detail of the probabilities (shown expanded), as predicted by the threshold (grey) and simple failure (dashed) models shown in Figures 1 and 2a.

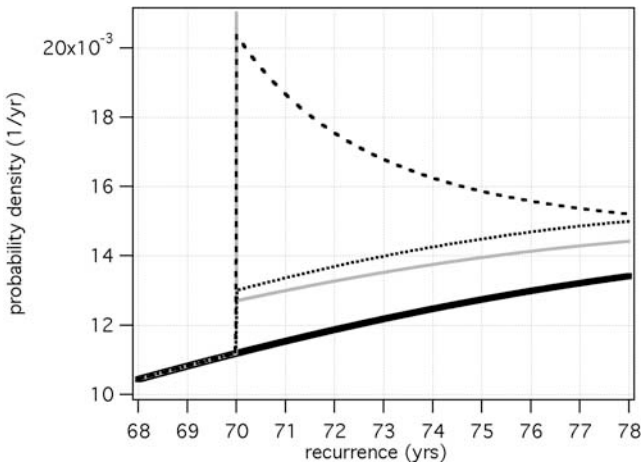

Figure 3. Log normal distribution of recurrence intervals with $\bar{l}_{t_r}$ = 4.6 ln(yr), s = 0.31 ln(yr) (black) shown with probability density for recurrence of a threshold model (grey) and a simple failure model [*Dieterich*, 1994] subject to a stress increase $\Delta\tau$ = 0.3 MPa, at t_0 = 70 yr, with $\dot{\tau}$ = 10 MPa/100 yr, b = 0.01, σ_n = 100 MPa, d_c = 5 μm and two choices of a, a = 0.005 (dashed) and a = 0.02 (dotted).

increased and the duration of the increase are controlled by the product $a\sigma_e$ [see *Dieterich*, 1994].

[5] Triggering of time-dependent earthquake rates as observed for aftershocks [*Mogi*, 1962; *Scholz*, 1968b; *Knopoff*, 1972; *Das and Scholz*, 1981; *Yamashita and Knopoff*, 1987; *Hirata*, 1987; *Reushle*, 1990; *Marcellini*, 1995, 1997; *Dieterich*, 1994; and *Gomberg et al.*, 2000 among others] and foreshocks [*Das and Scholz*, 1981; *Dieterich*, 1994] are predicted by the simple constitutive description [equation (3)]. Using an approach similar to equation (4) above, time-dependent earthquake probability can be estimated routinely for somewhat more sophisticated and realistic scenarios than our recurrence examples (Figures 1 and 2) [*Stein et al.*, 1997, *Toda et al.*, 1998; *Parsons et al.*, 2000; *Toda and Stein*, 2002; *Parsons*, 2002; *Gomberg et al.*, 2005]. However, there are pitfalls in using this lab observed behavior to calculate probability and triggering. First, rock friction results at temperatures less than 400°C suggest that a = 0.005 [e.g., *Beeler and Lockner*, 2003] to 0.039 [e.g., *Blanpied et al.*, 1998]. As the dependence of probability density on $a\sigma_e$ is nonlinear [equation (4)], this range produces remarkably different predictions in our recurrence example (Figure 3). σ_e could easily show a similar (factor of 8×) variation in the seismogenic portion of the crust. So earthquake occurrence can be said to be time-dependent as observed in the lab; yet, quantitative prediction based on lab values is suspect. Field based estimates of $a\sigma_e$ (0.4–1.2 MPa) are generally much lower than lab-predicted values [see summary by *Gomberg et al.*, 2000, p. 7862–7863]. Moreover, it is difficult to evaluate the value of $a\sigma_e$ for fault slip, given that the physical basis of this rate dependence in lab faulting experiments is not known. Second order instantaneous rate dependencies are ubiquitous in low temperature rock deformation: friction [*Dieterich*, 1979], fracture [*Scholz*, 1968a], crack growth [*Atkinson and Meredith*, 1987a, 1987b], and plasticity [*Mares and Kronenberg*, 1993]. So not knowing the mechanism responsible during earthquake faulting, we know little of how to extrapolate controlled lab observations to temperatures, pressures, fault mineralogy, and pore fluid chemistries of natural seismic fault zones.

[6] In this paper we examine the instantaneous rate dependence observed in a wide variety of laboratory experiments and in a variety of different rock types and find some instances where an underlying physical process of this rate dependence in rock friction tests can be tentatively identified. Using a normalization scheme modified from one proposed by *Tullis and Weeks* [1987] we address whether laboratory observations of the instantaneous rate dependence in rock friction are consistent with rate dependence measurements from higher temperature dislocation glide experiments. In addition, we show that the same normalization scheme can be used to compare rate dependence in friction to rock fracture and to low temperature crack growth tests.

2. Comparison Between Low Temperature Plasticity and Friction

[7] At constant strain rate and room temperature, some mineral phases, particularly weak phases such as phylosilicates can deform via dislocation glide (low temperature crystal plasticity). For glide, rock strength depends weakly and logarithmically on the strain rate; the rate dependence is well understood as a thermally activated process and the dislocation glide law [e.g., *Mares and Kronenberg*, 1993] has the Arrhenius form

$$\dot{\varepsilon} = \dot{\varepsilon}_* \exp\left\{-\frac{E_* - \sigma_\Delta \Omega}{kT}\right\}. \tag{5a}$$

If this flow law is expressed with strain rate as the independent variable, the observed differential strength is the sum of a nominal resistance and a rate-dependent term

$$\sigma_\Delta = \frac{E_*}{\Omega} + \frac{kT}{\Omega} \ln \frac{\dot{\varepsilon}}{\dot{\varepsilon}_*}, \tag{5b}$$

where σ_Δ is differential stress, E_* is the stress-free activation energy, Ω is the apparent activation volume and $\dot{\varepsilon}_*$ is a reference strain rate. The reference strain rate $\dot{\varepsilon}_*$ is not arbitrary, and E_*, Ω, and $\dot{\varepsilon}_*$ are determined experimentally from tests at multiple temperatures and strain rates. For purposes that will become clear in the following analysis, we wish to write equation (5b) with reference to an arbitrary strain rate that is proportional to $\dot{\varepsilon}_*$, $\dot{\varepsilon}_0 = c\dot{\varepsilon}_*$. Thus the nominal strength at $\dot{\varepsilon}_0$ is $\sigma_{\Delta 0} = E_*/\Omega + A_{\text{glide}} \ln c$ and we have

$$\sigma_\Delta = \sigma_{\Delta 0} + A_{\text{glide}} \ln\left(\dot{\varepsilon}^Y \Big/ \dot{\varepsilon}_0^Y\right) \tag{5c}$$

where the rate-dependent coefficient is $A_{\text{glide}} = kT/\Omega$.

[8] This rate dependence of low temperature plasticity is of the same form as the instantaneous rate dependence of rock friction [*Dieterich*, 1979], represented by the $a\ln V$ term in equation (3), and seen in rate stepping tests (Figure 4a–4b).

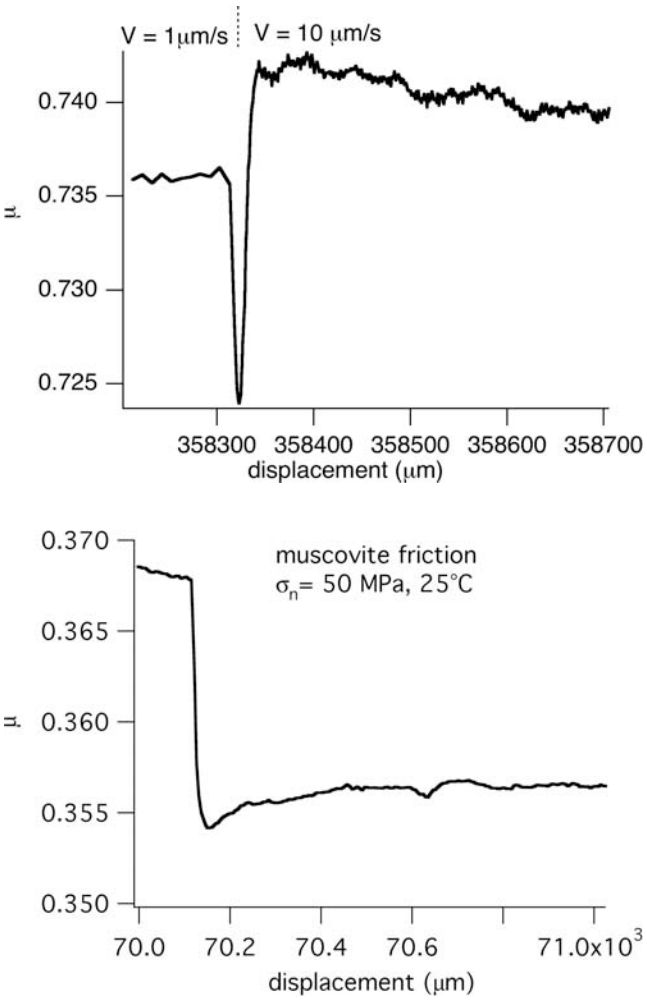

Figure 4. Examples of the instantaneous rate dependence of faulting. Rate stepping tests with a change in sliding velocity from 10 to 1 μm/s at constant normal stress from experiments on granite [*Beeler et al.*, 1996] and muscovite [*Scruggs and Tullis*, 1998]. In the case of granite, the instantaneous rate dependence is followed by a similar sized displacement dependent change of the opposite sense. For muscovite the displacement dependent effect is much smaller.

Rate stepping tests are well described by the rate and state friction equation

$$\mu = \mu_0 + a\ln(V/V_0) + b\ln(\theta/\theta_0) \tag{6}$$

[*Dieterich*, 1978, 1979; *Ruina*, 1983] of which equation (3) is a simplification appropriate for modeling the onset of rapid slip [*Dieterich*, 1992]. Given the common mathematical form, we may ask whether the instantaneous strain rate dependence of friction for some rocks is controlled by dislocation motion.

[9] At the outset, such friction and plasticity measurements are difficult to compare due to basic differences in the test configuration and conditions. There are the general differences in stress. Plasticity tests are typically conducted at higher confining pressure than rock friction tests and results are reported as differential stress on the sample versus strain rate, while rock friction results are reported as dimensionless shear resistance on a fault plane of known orientation versus slip rate. In addition, the inelastic process operating in plasticity experiments are distributed throughout the rock mass, while the processes resulting in rate dependence in rock friction tests are operating at very highly stressed contacting asperities across the fault. Consequently, the local ambient contact stresses depend on the specific asperity geometry. These contact stresses are not easily estimated from the macroscopic stress applied to the sample, and are generally unknown.

[10] In the following, we correct for differences in stress state and strain rate between different test configurations by appealing to basic aspects of friction theory. Our approach follows from *Tullis and Weeks* [1987] who recognized that the stress at asperity contacts was larger than the macroscopically applied stress approximately by the ratio of the nominal fault area to the real contacting area, and that differences in stress state can be removed by normalizing the data. We develop a normalization scheme that accounts for varying stresses and strain rates among different types of rock mechanics tests.

2.1. Rock Friction Theory

[11] In laboratory studies of frictional sliding on bare rock, sliding surfaces are typically machined flat and then roughened with grinding compound. The force applied normal to the plane F_n is concentrated at the relatively few asperity contacts across the roughened surfaces. What is generally observed is that, to first order, the ratio of macroscopically measured shear τ to normal stress σ_n is independent of normal stress. Friction theory assumes that the macroscopically observed resistance is due to resistance only at the asperity contacts. The average asperity normal stress is $\sigma_c = F_n/n\bar{A}_c$ where n is the number of contacts and $\bar{A}_c$ is the average asperity contact area. The macroscopic normal stress is $\sigma_n = F_n/A_T$ where A_T is the total fault plane area. Shear load F_s applied to the surface causes shear displacement, at an average contact shear strength $\tau_c = F_s/n\bar{A}_c$. The macroscopic shear stress is $\tau = F_s / A$. The shear stress $\tau = \tau_c\bar{A}_c / A_T$ and normal stress $\sigma_n = \sigma_c \bar{A}_c / A_T$ can be written without specific reference to the forces. If, as observed, the macroscopic ratio of shear stress to normal stress

$$\mu = \frac{\tau}{\sigma_n} = \frac{\tau_c}{\sigma_c} \tag{7a}$$

is approximately constant, the contact scale shear and normal stress ratio is also approximately constant.

[12] In addition to the first order friction resistance given by equation (7a), there are second order dependencies of friction on time of contact (age) and on slip velocity. Contact area increases slightly with time of contact due to small amounts of yielding at highly stressed asperity contacts [*Dieterich and Kilgore*, 1994]. However, because individual asperity contacts are very small relative to the total fault area, they have limited times of contact while the fault is sliding at a significant rate. Therefore any time-

dependent creep process operating at an asperity has a limited duration. While the contribution to resistance to slip of a single asperity may increase with time during static contact, there will be an ongoing reduction in the average asperity contact area due to shearing; after slip equivalent to the contact dimension, an asperity will no longer be in contact. So during slip there are two competing processes which determine the effective total contact area: time under load which tends to increase contact area, and slip which tends to replace yielding contacts bringing new, presumably, undeformed asperities into contact. This concept of competition between slip and time can be parameterized by considering the average age of the asperity contacts. For example, for constant slip rate V, average age takes the value $\bar{\theta} = d_c/2V$ where d_c is the representative length of the contacts on the fault surface. Conversely, during static contact $d\theta = dt$.

[13] These ideas have been incorporated into rock friction theory by allowing the asperity contact normal stress to be an explicit function of age θ,

$$\sigma_c = \sigma_0 + h(\theta) \tag{7b}$$

[*Dieterich*, 1979; *Linker and Dieterich*, 1992], where σ_0 is a reference value of contact stress and h is a function that decreases with age. Typically the dependence of friction on age is second order (for example, ~5% per decade change for granite at room temperature).

[14] For a fault sliding at steady state, an increase in sliding velocity produces the age-dependent effect equation (7b) and in addition an immediate increase in fault strength that scales with the size of slip rate change. The latter is the positive instantaneous rate-dependent effect that has been incorporated into friction theory by allowing the shear strength of asperity contacts to depend on sliding rate as

$$\tau_c = \tau_0 + g(V), \tag{7c}$$

[*Dieterich*, 1979; *Ruina*, 1983]. This effect is also second order (a few percent per decade change in slip rate is typical for granite at room temperature).

[15] The second order dependencies of fault strength on age and slip rate, equations (7b) and (7c), can be combined with equation (7a) into a relatively simple relation for friction

$$\mu = \frac{\tau}{\sigma_n} = \frac{[\tau_0 + g(V)]}{[\sigma_0 + h(\theta)]}\frac{[\sigma_0 - h(\theta)]}{[\sigma_0 - h(\theta)]}$$

Multiplying out the bracketed expressions in the numerator and denominator of the above expression and discarding the product of second order terms leads to the form of friction relation developed by *Dieterich* [1979] which is the basis of rate and state friction equations by *Ruina* [1983] and *Rice and Ruina* [1983]:

$$\mu = \frac{\tau_0}{\sigma_0} + \frac{g(V)}{\sigma_0} - \frac{\tau_0 h(\theta)}{\sigma_0^2}. \tag{8a}$$

On the right side of equation (8a), the first term is first order, the second term is the second order positive instantaneous dependence of contact shear resistance on sliding velocity, and the third term is the second order negative dependence of contact normal stress on contact age. Empirical expressions for the rate and age dependencies provide the remaining details of the rate and state formulation: $g(V) = A \ln (V / V_0)$ and $h(\theta) = \beta \ln(\theta / \theta_0)$. Expressing the first order term as $\tau_0 / \sigma_0 = \mu_0$, we have

$$\mu = \mu_0 + \frac{A \ln(V/V_0)}{\sigma_0} - \frac{\mu_0 \beta \ln(\theta/\theta_0)}{\sigma_0}. \tag{8b}$$

The rate and state constitutive equation (8b) can be expressed using more conventional notation as

$$\mu = \mu_0 + a \ln(V/V_0) + b \ln(V_0\theta/d_c) \tag{8c}$$

with coefficients $a = A / \sigma_0$, $b = -\mu_0\beta/\sigma_0$, $\theta_0 = d_c / V_0$, and d_c is a representative asperity contact dimension [*Dieterich*, 1979; *Ruina*, 1983]. The steady state value of age is $\theta_{ss} = d_c / V$ and the steady state value of friction is $\mu_{ss} = \mu_0 + (a - b) \ln V / V_0$.

2.2. Normalization Scheme

[16] To compare plasticity and rock friction results we eliminate differences in stress and strain rate. For friction, stress differences are accounted for by normalizing equation (8c) by the resistance μ_0 resulting from slip at the reference slip rate V_0 leading to

$$\frac{\mu}{\mu_0} = \frac{\tau_c \sigma_0}{\sigma_c \tau_0} = 1 + \frac{a}{\mu_0} \ln\frac{V}{V_0} + \frac{b}{\mu_0} \ln\frac{\theta}{\theta_0} \tag{9a}$$

[*Tullis and Weeks*, 1987]. Recalling the equivalences $a = A / \sigma_0$ and $b = -\mu_0\beta / \sigma_0$, we find that

$$\frac{\mu}{\mu_0} = 1 + \frac{A}{\tau_0} \ln\frac{V}{V_0} - \frac{\beta}{\sigma_0} \ln\frac{\theta}{\theta_0}. \tag{9b}$$

Note that there is no reference to the macroscopic stresses on the right side of equation (9b). The normalized coefficient of the rate-dependent term (A / τ_0) is the actual contact shear strength coefficient A, normalized by the stress driving shear deformation on the contact scale, the nominal contact shear strength τ_0.

[17] The same approach can be used to normalize the glide strength (5), resulting in

$$\frac{\sigma_\Delta}{\sigma_{\Delta 0}} = 1 + \frac{A_{glide}}{\sigma_{\Delta 0}} \ln\frac{\dot{\varepsilon}}{\dot{\varepsilon}_0}. \tag{10}$$

The normalized rate-dependent coefficient is the measured rate dependence divided by the nominal stress and has the same interpretation as that in equations (9a) and (9b), it is the rate dependence of the stress driving deformation, normalized by the ambient value of that stress. To compare the instantaneous rate-dependent coefficients the slip velocity in equation (10) must be converted to strain rate and the nominal strength must be determined at the same reference strain rate $\dot{\varepsilon}_0$ for equations (9a), (9b), and (10). Taking d_c from the friction relation to be one half of the average contact dimension, the strain rate for friction is $\dot{\varepsilon}_0 \approx V / 2d_c$.

Table 1. Rock Friction Data

Rock Type	μ_0	d_c (μm)	a	$\dot{\varepsilon}_0$, 1/s	a/μ_0	Reference
Granite	0.732	9.1	0.008	1×10^{-1}	0.011	*Beeler et al.* [1996]
Marble	0.773	9	0.0085	1×10^{-1}	0.011	*Tullis and Weeks* [1987]
Shale[a]	0.482	20	0.0052	1×10^{-1}	0.011	*Saffer and Marone* [2003]
Muscovite	0.364	125	0.0062	1×10^{-1}	0.017	*Scruggs and Tullis* [1998]
Talc	0.138–0.186	125	0.00335–0.0065	1×10^{-1}	0.024–0.035	*Scruggs* [1997]
Quartzite	0.705	1.3	0.0064	1×10^{-1}	0.009	*Weeks et al.* [1991]
Silica Glass	0.709	1.95	0.013	1×10^{-1}	0.018	*Weeks et al.* [1991]

[a]Data from inversions of rate steps at 2–20 μm/s, from Table 2 and Figure 4 of *Saffer and Marone* [2003].

2.3. Comparison of Rate Dependencies

[18] On the basis of a comparison between the rate dependence of frictional sliding of serpentinite at low sliding rates and the rate dependence for crystal plastic deformation of biotite single crystals at 400°C, *Reinen et al.* [1994] argued that dislocation glide is the mechanism underlying the rate dependence of serpentinite. Although *Escartin et al.* [1997] subsequently found no microstructural evidence of dislocation motion in serpentine rock failure tests at room temperature, the *Reinen et al.* [1994] argument may apply at asperity contacts on fault surfaces of other weak minerals known to deform by dislocation glide at room temperature, including biotite, muscovite, and illite, and also to strong materials that deform via dislocation motion at room temperature such as olivine [*Evans and Goetze*, 1979]. *Nakatani* [2001] has argued that some form of crystal plasticity controls the rate dependence of strong quartzofeldspathic rocks, but we are aware of no known instances of dislocation motion in these materials at room temperature. So we explore the idea of *Reinen et al.* [1994] that dislocation glide controls the friction rate dependence using nonquartzofeldspathic materials at room temperature. In comparing rate dependencies of friction and low temperature plasticity, the *Tullis and Weeks* [1987] approach taken by *Reinen et al.* [1994] makes implicit use of equations (9a), (9b), and (10) but they did not account for the dependence of the rate-dependent coefficient in equation (10) on temperature and they did not attempt to convert frictional slip rate to contact strain rate so that rate dependencies of friction and distributed deformation are compared at equivalent rates.

[19] We compare friction and dislocation glide data for muscovite and talc; results are summarized in Table 1 (friction) and Table 2 (glide). Microstructural analysis of muscovite single crystals deformed with σ_1 at 45° to the 001 plane, at pressure between 50 and 400 MPa and temperatures between 20° and 400°C indicates deformation predominately by dislocation glide [*Mares and Kronenberg*, 1993]. Analysis of these 400°C rate stepping experiments (Figure 6) for $\dot{\varepsilon}_0 = 1 \times 10^{-1}$ gives a normalized coefficient of rate dependence of dislocation glide equal to $A_{\text{glide}} / \sigma_{\Delta 0} = 0.034$ (Figure 5). Note that there is variability in the strength and rate dependence, thus their ratio has significant uncertainty. To compare with room temperature friction data, the difference in temperature (673 to 295 K) introduces a reduction in A_{glide} of a factor of 2.3 for the single crystal glide data. The *Mares and Kronenberg* [1993] single crystal data extrapolated to room temperature yield $A_{\text{glide}}/\sigma_{\Delta 0} = 0.015$.

[20] The normalized coefficient of rate dependence from room temperature friction tests for muscovite [*Scruggs and Tullis*, 1998] is estimated using equations (9a) and (9b) but there is some ambiguity in the strain rate. These experiments were conducted on 1-mm thick layers of powdered muscovite rather than bare rock surfaces where slip is known to be localized. If the deformation is distributed within the layer the characteristic distance d_c is related both to the average contact dimension and the thickness of the actively deforming layer [*Marone and Kilgore*, 1993]. In the case of these particular experiments, the inferred value of $d_c = 125$ μm from rate stepping tests is quite a bit larger than d_c in the granite bare surface experiments, consistent with distributed deformation. Fortunately, the normalization scheme is insensitive to differences in strain rate of this magnitude; if we use a range $d_c = 9$ to 125 μm, μ_0 varies from 0.359 to 0.372 and we find $A / \tau_0 = 0.017$ for either choice. This normalized rate dependence is similar to the single crystal glide value suggesting that the instantaneous rate dependence in muscovite could well be related to dislocation motion. Note if glide controls the instantaneous rate dependence of friction, the rate coefficient should scale linearly with temperature, as envisioned in recent process-based rock friction theories [e.g., *Rice et al.*, 2001, *Nakatani*, 2001] and observed in the experiments of *Nakatani* [2001].

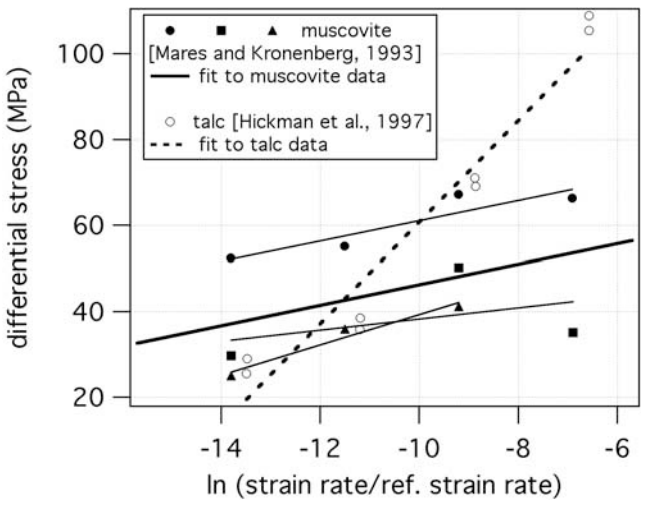

Figure 5. Rate dependence due to dislocation glide in muscovite and talc at 400°C. These are from rate stepping tests on muscovite at 200 MPa confining pressure [*Mares and Kronenberg*, 1993] and talc at 300 MPa [*Hickman et al.*, 1997].

Table 2. Glide Data

Rock Type	$\sigma_{\Delta 0}$, MPa	A, MPa	$\dot{\varepsilon}_0$, 1/s	$A/\sigma_{\Delta 0}$	Reference
Muscovite[a]	70	1.05	1×10^{-1}	0.015	*Mares and Kronenberg* [1993]
Talc[b]	179	5.2	1×10^{-1}	0.029	*Hickman et al.* [1997]

[a]Average of three experiments at 400°C, 200 MPa confining pressure, A is corrected to room temperature.
[b]Average of two experiments at 400°C, 300 MPa confining pressure, A is corrected to room temperature.

[21] In low velocity friction tests on serpentinite, *Reinen et al.* [1994] observed a transition to a more strongly rate-dependent process that they tentatively identified as glide. Similar low velocity rate stepping and hold tests on muscovite do not seem to produce such a transition and the rate dependence in the velocity range 0.001 to 10 μm/s is approximately constant. Our preliminary conclusion is that dislocation glide is responsible for the instantaneous rate-dependent effect in muscovite friction at all laboratory slip rates.

[22] Similar analysis is possible for talc using deformation data for intact polycrystalline samples from *Hickman et al.* [1997] and friction tests of *Scruggs* [1997]. The intact polycrystalline experiments were conducted at pressures between 50 and 400 MPa and temperatures between 20° and 600°C. Analysis of 400°C rate stepping experiments, again taking $\dot{\varepsilon}_0 = 1 \times 10^{-1}$, produces a normalized coefficient of rate dependence of $A / \sigma_{\Delta 0} = 0.066$ (Figure 5). The value of A must again be corrected to room temperature to be compared with the friction data; using the same procedure, we find $A / \sigma_{\Delta 0} = 0.029$ at ambient conditions. The normalized coefficient of rate dependence from two room temperature friction tests for talc gouge is estimated as before and we find $A / \tau_0 = 0.024$ to 0.035. This value bounds the polycrystalline value suggesting that the friction instantaneous rate dependence could well result from the same mechanism controlling the deformation in the intact polycrystalline experiments. Though *Hickman et al.* [1997] did not do microstructural analysis on their samples, observations of dislocations within the basal interlayers of talc [*Amelinckx and Delavignette*, 1962] indicate that easy glide is readily activated at room temperature. The dependence determined from intact polycrystalline samples is thus interpreted to represent glide.

3. Instantaneous Rate Dependence of Brittle Rock Failure

[23] In low temperature, constant strain rate experiments performed on crystalline rocks peak strength prior to fracture and strength during brittle yielding depend weakly and logarithmically on the strain rate approximately following an empirical relationship identical to equation (5c)

$$\hat{\sigma}_\Delta = \hat{\sigma}_{\Delta 0} + \hat{A} \ln(\dot{\varepsilon}/\dot{\varepsilon}_o) \tag{11a}$$

[e.g., *Heard*, 1963; *Rutter*, 1974; *Lockner*, 1998] (Figure 6). It is widely argued that subcritical crack growth underlies the rate dependence of low temperature failure in crystalline rock equation (11a) [e.g., *Scholz*, 1968a], but in some materials there may be contributions from plasticity or other mechanisms.

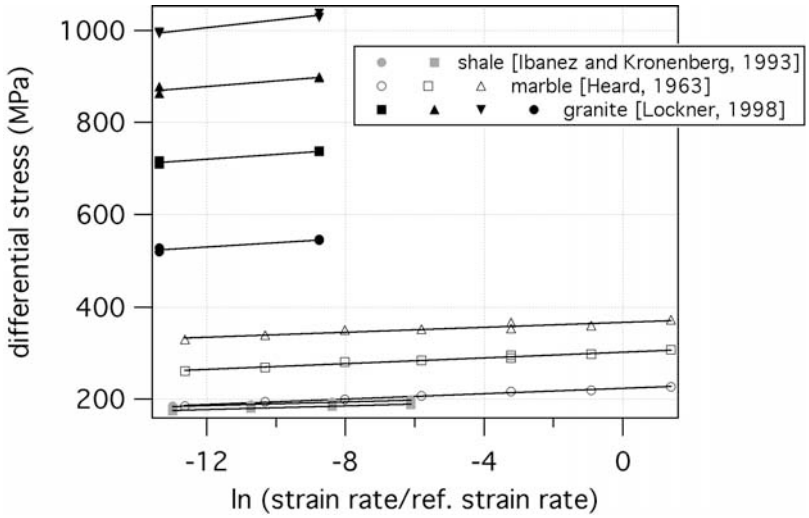

Figure 6. Instantaneous rate dependence of intact rock strength. The granite data of *Lockner* [1998] represent peak stresses from different experiments at different strain rates for 50, 100, 150, and 200 MPa confining pressure. The marble data of *Heard* [1963] represent strength from different experiments at different strain rates measured at 2, 5, and 10% strain, all data at 500 MPa confining pressure. The shale data of *Ibanez and Kronenberg* [1993] reflect changes in stress due to strain rate steps for single experiments at 250 MPa confining pressure. In all cases the reference strain rate is 1×10^{-1}/s.

Table 3. Brittle Intact Rock Data

Rock Type	$\sigma_{\Delta 0}$, MPa	A, MPa	$\dot{\varepsilon}_0$, 1/s	$A/\sigma_{\Delta 0}$	Reference
Granite[a]	857	6.1	1×10^{-1}	0.007	*Lockner* [1998]
Marble[b]	298	2.95	1×10^{-1}	0.010	*Heard* [1963]
Shale[c]	205	1.99	1×10^{-1}	0.010	*Ibanez and Kronenberg* [1993]

[a]Room temperature experiments, stress measured at peak, for data at 50, 100, 150, and 200 MPa confining pressure; data are averaged.
[b]Room temperature experiments, stress measured at 2, 5, and 10%, at 500 MPa; data are averaged.
[c]Room temperature experiments at 250 MPa confining pressure, deformed with σ_1 45° to bedding.

3.1. Normalization

[24] For the moment, we assume that the observed behavior described by equation (11a) is controlled by an unknown underlying rate-dependent deformation mechanism that has a material yield strength τ_y and that for any particular set of conditions (temperature and stress) the observed differential stress is proportional to the yield strength, for example, $\hat{\sigma}_\Delta = C\tau_y$. The coefficient C can be considered to be like the reciprocal of a stress intensity factor that simply relates the macroscopically applied stress to the yield stress. As it is well known that both strength [equation (11a)] and rate dependence increase with confining pressure in brittle rock failure tests [e.g., *Lockner*, 1998], by assuming that τ_y is a material property we are implicitly assuming that C increases with confining pressure. Under these assumptions we write yield strength as

$$\tau_y = \tau_{y0} + A \ln(\dot{\varepsilon}/\dot{\varepsilon}_0) \tag{11b}$$

where $\tau_{y0} = \sigma_{\Delta 0} / C$ and $A = \hat{A}/C$ .The significant difference between equations (11b) and (11a) is that τ_{y0} and A are assumed material constants associated with some process of yielding on the microscopic scale, whereas $\hat{\sigma}_{\Delta 0}$ and $\hat{A}$ are macroscopically observed pressure-dependent coefficients.

[25] Applying the normalization scheme developed in section 2.2 to equation (11b) we find

$$\frac{\tau}{\tau_{y0}} = 1 + \frac{A}{\tau_{y0}} \ln(\dot{\varepsilon}/\dot{\varepsilon}_0) = \frac{\hat{\sigma}_\Delta}{\hat{\sigma}_{\Delta 0}} = 1 + \frac{\hat{A}}{\hat{\sigma}_{\Delta 0}} \ln(\dot{\varepsilon}/\dot{\varepsilon}_0). \tag{11c}$$

As before, the normalization produces equivalence between the normalized macroscopically observed rate dependence and the rate dependence associated with the underlying process. Namely, the measured rate dependence divided by the nominal stress is the rate dependence of the stress driving deformation on the microscopic scale, normalized by the ambient value of that stress. In addition, when comparing equation (11c) with equations (9a) and (9b), geometric differences between measured differential stress σ_Δ in rock failure tests and shear stress in friction tests ($\tau = 0.5\sigma_\Delta \sin 2\beta$ where β is the angle between the fault normal and the greatest principal stress) are also eliminated.

3.2. Comparison of Rate Dependencies

[26] We compare the instantaneous rate dependence of rock failure with that of friction for some representative crustal rock types, granite, marble, and shale using equation (11c) and equations (9a) and (9b). The rate dependence of rock failure data for these different materials is shown in Figure 6. The resulting values are listed in Tables 1 and 3. Both intact failure tests and friction yield values of the normalized rate-dependent coefficient in the range 0.007 to 0.011 for granite at room temperature. We consider these to be identical given the approximate nature of the comparison. Even better agreement is found for the rate dependence for marble, with a range 0.01 to 0.011. For shale the range is also narrow, from 0.01 to 0.011. Our normalization of friction and intact failure is a formal version of *Tullis and Weeks* [1987] who concluded that a common mechanism was responsible for the instantaneous rate dependence in carbonate rock fracture and friction.

[27] In the case of granite, the similarity between rock failure and rock friction rate dependencies was previously noted by *Lockner* [1998] who compared normalized fracture rate dependence $d\sigma_\Delta/\sigma_\Delta d\dot{\varepsilon}$ to a from friction tests of *Blanpeid et al.* [1998]. Though Lockner's approach does not normalize the friction data and does not consider differences in strain rate, these differences have little effect on the outcome. These data are somewhat insensitive to differences in strain rate because of the logarithmic dependence and the small rate coefficient. As the friction coefficient is near 1 not normalizing by it makes little difference and Lockner concluded, as we have, that the same physics underlies the instantaneous rate dependence of friction and rock failure in granite.

4. Crack Growth and Friction

[28] Many studies since *Scholz* [1968a] have argued or assumed that the rate dependence of rock fracture strength is related to the growth rate-dependence of individual tensile cracks in double cantilever experiments such as those on glass [e.g., *Lawn*, 1993] and single mineral crystals [e.g., *Atkinson*, 1984]. A common argument in the brittle rock mechanics literature is that precursory (secondary creep) and volumetric strain observed in rock failure tests [*Scholz*, 1968a; *Lockner*, 1998] result from the collective growth of many initially subcritical cracks. Figure 7 shows examples of "subcritical" crack growth, including data from single cracks propagating in quartzofeldspathic materials, marble [*Atkinson and Meredith*, 1987a, 1987b], and fused silica glass [*Lawn*, 1993]. The horizontal axis is crack propagation velocity and the vertical axis is the stress intensity factor K_i; stress intensity is related to the remotely applied driving stress σ and to the crack length c as $K_i \propto \sigma\sqrt{c}$. Fortunately, crack growth experiments (Figure 7) are commonly done using a geometry where K_i is independent of crack dimensions and thus [*Atkinson and Meredith*, 1987b], and the crack length dependence can be ignored. As shown, subcritical crack growth has a nonlinear viscous rheology; as the stress on the sample increases crack velocity increases, or alternatively, as the crack propagation velocity increases, the crack strength increases. Subcritical crack growth in minerals is generally similar to that in glass and, at comparable temperature, crystalline materials (quartz) are somewhat stronger than their amorphous counterparts (fused silica). Though not shown in Figure 7, there is a measurable temperature dependence to crack growth [*Atkinson and Meredith*, 1987a, 1987b], indicating that a thermally activated mechanism controls growth.

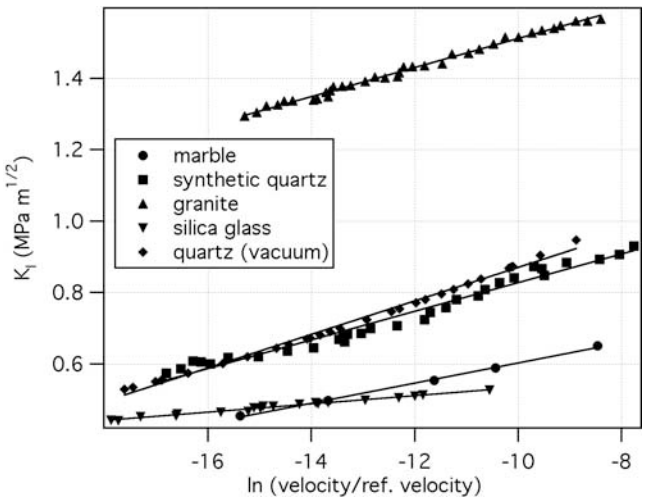

Figure 7. Rate dependence of subcritical crack growth in quartzofeldspathic materials, silica glass, and marble at room temperature. The vertical axis is stress intensity which is proportional to stress. With exception of the synthetic quartz in vacuum (diamonds), all experiments were conducted in the presence of liquid or atmospheric water. The source references for these experiments are listed in Table 4. The normalizing velocity used is 1 m/s (1×10^6 μm/s).

[29] For well-studied minerals and for other brittle materials, it is widely held that subcritical crack propagation rate depends on a chemically reactive environment, and rates are determined by the chemical reaction at the crack tip [i.e., the rate at which bonds are broken; *Charles and Hillig*, 1962; *Atkinson and Meredith*, 1987a, 1987b]. This particular type of subcritical crack growth is known as stress corrosion, and has a crack tip velocity v with an Arrhenius dependence on stress and temperature:

$$v = v_0 \exp\left(\frac{-E + \Omega\sigma_t - \Omega_m\Gamma/\rho}{RT}\right) \tag{12a}$$

[*Charles and Hillig*, 1962] where E is the stress free activation energy, Ω is the activation volume, Ω_m is molar volume, Γ is the interfacial energy, R is the gas constant, and ρ is the radius of curvature at the crack tip.

4.1. Normalization

[30] Direct comparison between the rate dependence of subcritical crack growth and that of rock friction can be made following the procedure outlined previously. Because subcritical crack growth occurs in a vacuum as well as in the presence of water (Figure 7), rather than use the Charles and Hillig equation, which is specific to water-assisted crack growth (stress corrosion), we use a more general, Arrhenius form

$$v = v_0 \exp\left(\frac{-E_0 + \varsigma K_i}{RT}\right) \tag{12b}$$

where is an empirical constant and E_0 is an activation energy [*Wiederhorn and Bolz*, 1970; *Wiederhorn*, 1978]. Expressing this relationship with crack velocity v as the independent variable and the macroscopic stress as the dependent variable leads to

$$\sigma \propto \left\{\frac{E_0}{\varsigma} + \frac{RT}{\varsigma}\ln\frac{v}{v_0}\right\} \tag{12c}$$

We normalize this expression by the applied stress σ_0 that results in crack propagation at rate v_0;

$$\frac{\sigma}{\sigma_0} = 1 + \frac{RT}{E_0}\ln\frac{v}{v_0} \tag{12d}$$

Note that the rate-dependent term in equations (12a), (12b), (12c), and (12d) is analogous to that in equations (9a) and (9b); it is the rate dependence of the remotely applied stress driving crack propagation, divided by the nominal value of that stress. In addition to eliminating the unknown ζ, an unknown constant of proportionality relating stress to stress intensity is eliminated by the normalization. Related analysis and comparison between crack growth and friction was undertaken by *Kato et al.* [1993].

4.2. Comparison of Rate Dependencies

[31] To compare the crack growth experiments as described by equations (12a), (12b), (12c), and (12d) to friction data as described by equations (9a) and (9b) or to rock failure data as described by (11c) the rate of crack propagation v must be equated with the fault slip rate V or with fault zone strain rate. Lab fault slip rates and crack growth rates are very different in magnitude. The upper limit of friction rate stepping tests velocity may reach 1 to 10 μm/s while crack growth rates reach 1×10^{-2} m/s. If we equate v directly to V, implying that frictional slip produces crack growth at the same rate, and choose a reference velocity of 1.8 μm/s, the ratio $RT/E_0 = 0.055$ from equations (12a), (12b), (12c), and (12d) for marble does not compare favorably with the analogous friction parameter $a / \mu_0 = 0.011$. With the same assumption (of $v = V$) a discrepancy of similar size is noted for quartz, granite, and silica glass. This discrepancy might be due to very large differences in the true rate of crack growth from that assumed at a particular fault sliding velocity. However, the crack velocity necessary to account for the discrepancy in normalized rate dependence appears to be unreasonably large and of the opposite sense to our expectation, as follows. One would expect that frictional slip produces many cracks at asperity contacts such that the average rate of growth of a representative crack is smaller than the slip rate. However, to reduce RT/E_0, E_0 must be larger. Since crack growth has a positive rate dependence, larger values of E_0 correspond to larger values of the reference velocity v_0, rather than smaller values. To produce a normalized rate dependence of crack growth similar to that seen in the friction experiments, the reference velocity must greatly exceed the compressive wave speed. Obviously, frictional slip can not produce subcritical crack growth at asperity contacts with a propagation velocity approaching the elastic wave speed.

[32] To estimate the normalized rate dependence of crack growth in geologic materials, we arbitrarily allow that the crack growth during laboratory friction experiments occurs

Table 4. Crack Growth Data

Rock Type	E_0/ξ	RT/ξ	v_0, μm/s	RT/E_0	Reference
Granite	1.92	0.041	1×10^6	0.021	*Meredith and Atkinson* [1985]
Marble	0.886	0.028	1×10^6	0.032	*Atkinson* [1984]
Synthetic Quartz (Vacuum)	1.34	0.047	1×10^6	0.035	*Meredith and Atkinson* [1982]
Synthetic Quartz	1.23	0.040	1×10^6	0.032	*Meredith and Atkinson* [1982]
Silica Glass	0.650	0.012	1×10^6	0.018	*Lawn* [1993]

at subcritical rates of 1 m/s (v_0 in (12) is 1 m/s). This is about one order of magnitude higher than the largest rates in typical subcritical crack growth experiments. Results are summarized in Table 4 for comparison with Tables 1 and 3. Silica glass has a normalized crack growth rate dependence of $RT/E_0 = 0.018$ [*Lawn*, 1993], which is identical to the normalized friction rate dependence of $a/\mu_0 = 0.018$ in silica glass [*Weeks et al.*, 1991]. This result may seem satisfying; however, the friction data are poor quality. The normalized rate dependence of subcritical crack growth in Westerly granite at room temperature is $RT/E_0 = 0.021$ [*Atkinson and Meredith*, 1987a] while the analogous normalized rate-dependent coefficient from Westerly granite friction tests is only $a/\mu_0 = 0.011$ [e.g., *Beeler et al.*, 1996], roughly one half the crack growth value. This result is consistent with that of *Kato et al.* [1993] who used a somewhat different approach and found crack growth in granite to have larger direct rate dependence than granite friction. The normalized rate-dependent coefficient from room temperature experiments on synthetic quartz in water and in vacuum are 0.032 to 0.035 [*Meredith and Atkinson*, 1982], while the coefficient from quartzite friction tests is 0.009 [*Weeks et al.*, 1991], less than one third the crack growth value. Essentially identical results are found for marble; for crack growth the normalized rate dependence at room temperature is 0.032 while the normalized friction data of *Tullis and Weeks* [1987] exhibits a rate dependence of 0.011, again about one third the crack growth value. We conclude that quartzofeldspathic rocks and marble show rate dependencies that are not consistent with crack growth. While there is great uncertainty in the proper reference crack velocity to use in comparisons of friction and crack growth data, the difference can not be reconciled by adjustments in the rates chosen as the reference.

5. Discussion

[33] Determining the deformation mechanisms underlying the instantaneous rate dependence of natural seismic faulting is our primary goal. To this end, the study is a limited success. While we infer that dislocation glide underlies friction rate dependence of talc and muscovite, these minerals are rate strengthening and incapable of sustaining rapid earthquake slip. Those particular results may have implications for the mechanics of fault creep, but have no apparent relevance to natural seismicity. Our most significant result for studies of earthquake occurrence and earthquake probability is finding that for particular rock types friction and rock failure rate dependencies are essentially identical. If this proves to be a general result, modeling of time-dependent failure, earthquake probability, and time-dependent seismic hazard in different settings (for example, mature fault zones, unfaulted rock), can be represented by the same rock-type specific material constant.

[34] Our comparison of crack rate and friction rate dependencies does not support arguments that crack growth controls the instantaneous rate dependence of rock friction and fracture in quartzofeldspathic rock [e.g., *Scholz*, 1968a, 1968b; *Lockner*, 1998]. In all cases, the crack growth rate dependencies are larger than the instantaneous rate dependence determined for friction. Arguably, subcritical crack growth occurs in all instances of natural faulting in the shallow crust, in laboratory rock fracture tests and in friction experiments, as indicated by pervasive dilatant and shear microcracks, macroscopic fracture, and wear material (gouge) that accompany frictional sliding. The disagreement between faulting and crack growth experiments is particularly hard to understand.

[35] If fracture and friction instantaneous rate dependencies in quartzofeldspathic rocks and carbonates are controlled by the physics of crack growth, crack growth rates must be called upon that differ from those that have been measured experimentally. Subcritical crack growth may be controlled by reaction rates, or diffusion rates and these regimes may be defined. All subcritical crack growth data used in our comparison have been collected in the reaction-controlled regime. Diffusion-controlled regime 2 crack growth shows a higher rate dependence than regime 1, and probably will more poorly match rate dependencies of friction. At lower (regime 0) and higher crack growth rates (regime 3), the expected rate dependencies can be lower than in regime 1 [*Atkinson and Meredith*, 1987a]. Another possible difference between crack growth experiments and typical rock fracture and friction tests might be the crack propagation mode. All the subcritical crack growth data are for the tensile growth, mode I, whereas rock fracture and rock friction tests may involve mixed mode fracturing. As the rate dependencies of crack extension in modes II and III or mixed modes have not been measured for rocks and minerals, appropriate values for comparison are not available.

[36] Somewhat independent of the success of this particular study, as summarized by specific comparisons in Tables 1–4, the normalization scheme can produce an estimate of the activation energy underlying the instantaneous rate dependence. For example, the case of dislocation glide equation (10) with normalized rate dependence $A_{\text{glide}} / \sigma_{\Delta 0} = kT/(E^* + kT \ln c)$. If the reference strain rate is chosen as $\dot{\varepsilon}_0 = \dot{\varepsilon}_*$, then $A_{\text{glide}} / \sigma_{\Delta 0} = kT/E^*$, and the ratio will directly reflect the process activation. So if the same reference strain rate is used to normalize the friction data, and the friction instantaneous rate dependence is controlled by dislocation glide, the ratio a/μ_0 directly reflects the activation energy [also see *Nakatani*, 2001]. Because activation energies for glide are typically 20 or more times larger than kT, the method is forgiving in that the choice of reference strain rate need not be exact. Similar, results might be possible for crack growth. However, the success relies on knowing the proper reference within a couple of orders of

magnitude which will be difficult without already knowing the deformation mechanism. We conclude that inferring activation energy from the normalized data is not an adequate alternative to direct measurements such as temperature stepping tests.

6. Conclusions

[37] The rate dependence of rock failure strength and the instantaneous rate dependence of friction are consistent for three different rocks considered: a strong quartzofeldspathic material (granite), an intermediate strength carbonate (marble), and for a weak clay-rich material (illite-bearing shale). These results suggest that the physics controlling the instantaneous rate-dependent brittle behavior in rock failure and rock friction of these materials are the same. The instantaneous rate dependence of room temperature friction for two weak phases, mica and talc, are consistent with higher temperature experiments on these minerals where deformation is accommodated by dislocation glide. However, the room temperature instantaneous frictional rate dependence of stronger materials, quartz, granite, and marble are not quantitatively consistent with available room temperature data from crack growth, suggesting that the instantaneous frictional rate dependence for strong, brittle rocks does not involve crack growth. We view this as unlikely but have not reconciled the discrepancy.

Appendix A: Recurrence Probability Density

[38] We calculate earthquake recurrence probability density using a log normal distribution

$$P(t_r) = \frac{1}{s t_r \sqrt{2\pi}} \exp\left(-\left[\ln t_r - \bar{l}_{t_r}\right]^2 \Big/ 2s^2\right) \tag{A1}$$

where t_r is recurrence interval, $\bar{l}_{t_r}$ is the average log recurrence interval and s is the standard deviation of log recurrence interval (Figure 1, black). $P(t_r)$ is the unperturbed probability density, the probability distribution in the absence of a triggering stress change. The stressing rate $\dot{\tau}$ is assumed to be constant.

[39] For time-dependent failure we use an earthquake occurrence rate formulation [*Beeler and Lockner*, 2003], that is a generalization of *Dieterich*'s [1994] approach, [also see *Gomberg et al.*, 2000] to determine how stress changes the earthquake probability density. Note that probability density is a normalized recurrence rate having units time^{-1}. Thus there is a direct proportionality between probability density and earthquake rate $r = \mathrm{d}n/\mathrm{d}t_r$

$$r(t_r) = n_T P(t_r) \tag{A2}$$

where n is the event number and n_T is the total number of events. For a recurring earthquake with a known, bounded probability density, both the unperturbed ($P(t_r)$) and perturbed ($P(t)$) probability densities must satisfy $\int_0^\infty P(t)\mathrm{d}t = \int_0^\infty P(t_r)\mathrm{d}t_r = 1 = n_T$ and the total number of events is one. So rate and probability density are equivalent. The rate of recurrence in the absence of a static stress change above the background stressing is $r(t_r) = \Delta n / \Delta t_r$ where t_r is the unperturbed recurrence time. Following a stress change, the recurrence time may be increased or decreased by an amount $t_c = t_r - t$ where t_c is the clock advance (positive values indicate that recurrence time is advanced [*Gomberg et al.*, 1998]), and t is the recurrence time due to the constant stressing and the static stress change. Using this choice of variables the unperturbed recurrence rate is $r(t_r) = \Delta n/(\Delta t_c + \Delta t_r)$. Defining the perturbed recurrence rate as $r(t) = \Delta n / \Delta t$, the reciprocal rate as a function of time is

$$\frac{1}{r}(t) = \frac{1}{r(t_r)} - \frac{\Delta t_c}{\Delta n}(t). \tag{A3}$$

[see *Gomberg et al.*, 2000; *Beeler and Lockner*, 2003 for more details]. Expressing this as a seismicity rate, recasting the differences as differentials, and equating with probability density using equation (A2), we have

$$P(t) = \frac{P(t_r)}{1 - \dfrac{\mathrm{d}t_c}{\mathrm{d}t_r}(t)}. \tag{A4}$$

Equation (A4) can be used with any fault failure relation for which the clock advance due to stress change can be estimated. A simple rock fracture and stick-slip friction failure stress was proposed by *Dieterich* [1992, 1994]: $\frac{\tau}{\sigma_e} = \mu_* + a \ln \frac{V}{V_*} - b \frac{\delta}{d_c}$ [see text below equation (3)]. Assuming constant fault normal stress, for a shear stress change of size $\Delta\tau$ imposed at t_0, the change in recurrence time is

$$t_c = \begin{array}{ll} 0 & t_r < t_0 \\ \frac{\Delta\tau}{\dot{\tau}} - \frac{a\sigma_e}{\dot{\tau}} \ln\left\{1 - \exp\left(\dot{\tau}t_0 \Big/ a\sigma_e\right)\right][1 - \exp\left(\Delta\tau \Big/ a\sigma_e\right)] \exp\left(-\dot{\tau}t_r \Big/ a\right)\Big\} & t > t_0 \end{array} \tag{A5}$$

[*Gomberg et al.*, 1998] and $t = t_r - t_c$. Using this solution to calculate the derivative $\mathrm{d}t_c / \mathrm{d}t_r$, and using that relation with the log normal distribution of failure times we have recurrence probability density due to static stress change:

$$P(t) = \begin{array}{ll} \frac{1}{st\sqrt{2\pi}} \exp\left(-\left[\ln(t) - \bar{l}_{t_r}\right]^2 \Big/ 2s^2\right) & t < t_0 \\ \frac{\frac{1}{s(t+t_c)\sqrt{2\pi}} \exp\left(-\left[\ln(t+t_c) - \bar{l}_{t_r}\right]^2 \Big/ 2s^2\right)}{1 + [\exp(-\Delta\tau/a\sigma_e) - 1] \exp[-\dot{\tau}(t - t_0)/a\sigma_e]} & t \geq t_0 \end{array} \tag{A6}$$

The formulation developed in this Appendix is also discussed in the separate paper by *Gomberg et al.* [2005], and is equivalent to the numerical scheme of *Hardebeck* [2004].

[40] **Acknowledgments.** The earthquake probability approach shown in Figures 1, 2, and 3 and included in the Appendix was developed in collaboration with Joan Gomberg. Masao Nakatani corrected a serious error

in our original analysis of rock fracture data and pointed out the earlier paper on friction and crack growth by N. Kato and others. Discussion and correspondence with J. D. Weeks, T.-F. Wong, G. Hirth, and particularly D. Lockner and M. Nakatani are gratefully acknowledged. This research was supported by the US Geological Survey and the Southern California Earthquake Center. This is SCEC contribution 1020.

References

Amelinckx, S., and P. Delavignette (1962), Dislocations in layer structures, in *Direct observations of imperfections in crystals*, edited by J. B. Newkirk and J. H. Wernick, pp. 295–356, Wiley-Interscience, Hoboken, N. J.

Atkinson, B. K. (1984), Subcritical crack growth in geologic materials, *J. Geophys. Res.*, *89*, 4077–4114.

Atkinson, B. K., and P. G. Meredith (1987a), The theory of subcritical crack growth with applications to minerals and rocks, in *Fracture Mechanics of Rock*, edited by B K. Atkinson, pp. 111–166, Elsevier, New York.

Atkinson, B. K., and P. G. Meredith (1987b), Experimental fracture mechanics data for rocks and minerals, in *Fracture Mechanics of Rock*, edited by B. K. Atkinson, pp. 477–525, Elsevier, New York.

Beeler, N. M., and D. A. Lockner (2003), Why earthquakes correlate weakly with the solid Earth tides, *J. Geophys. Res.*, *108*, (B8), 2391, doi:10.1029/2001JB001518.

Beeler, N. M., T. E. Tullis, M. L. Blanpied, and J. D. Weeks (1996), Frictional behavior of large displacement experimental faults, *J. Geophys. Res.*, *101*(B4), 8697–8715.

Blanpied, M. L., C. J. Marone, D. A. Lockner, J. D. Byerlee, and D. P. King (1998), Quantitative measure of the variation in fault rheology due to fluid-rock interactions, *J. Geophys. Res.*, *109*, 9691–9712.

Charles, R. J., and W. B. Hillig (1962), The kinetics of glass failure by stress corrosion, in Symposium sur la resistance due verre et les moyens de l'ameliorer, pp. 511–527, Union Scientific Continentale du Verr, Charleroi, Belgium.

Das, S., and C. H. Scholz (1981), Theory of time-dependent rupture in the Earth, *J. Geophys. Res.*, *86*, 6039–6051.

Dieterich, J. H. (1978), Time-dependent friction and the mechanics of stick slip, *Pure Appl. Geophys.*, *116*, 790–806.

Dieterich, J. H. (1979), Modeling of rock friction: 1. Experimental results and constitutive equations, *J. Geophys. Res.*, *84*, 2161–2168.

Dieterich, J. H. (1992), Earthquake nucleation on faults with rate- and state-dependent strength, in *Earthquake Source Physics and Earthquake Precursors*, edited by T. Mikumo et al., pp. 115–134, Elsevier, New York.

Dieterich, J. H. (1994), A constitutive law for rate of earthquake production and its application to earthquake clustering, *J. Geophys. Res.*, *99*, 2601–2618.

Dieterich, J. H., and B. D. Kilgore (1994), Direct observation of frictional contacts: New insights for state-dependent properties, *Pure Appl. Geophys.*, *143*, 283–302.

Escartin, J., G. Hirth, and B. Evans (1997), Nondilatant brittle deformation of serpentinites: Implications for Mohr-Coulomb theory and the strength of faults, *J. Geophys. Res.*, *102*, 2897–2913.

Evans, B., and C. Goetze (1979), The temperature variation of hardness of olivine and its implication for polycrystalline yield stress, *J. Geophys. Res.*, *84*, 5505–5524.

Gomberg, J. (2001), The failure of earthquake failure models, *J. Geophys. Res.*, *106*, 16,253–16,264.

Gomberg, J., N. M. Beeler, M. L. Blanpied, and P. Bodin (1998), Earthquake triggering by transient and static deformations, *J. Geophys. Res.*, *103*, 24,411–24,426.

Gomberg, J., N. M. Beeler, and M. L. Blanpied (2000), On rate-state and Coulomb failure models, *J. Geophys. Res*, *105*, 7857–7871.

Gomberg, J., P. Reasenberg, M. Cocco, and M. E. Bardinelli (2005), Time-dependent earthquake probabilities based on population models, *J. Geophys. Res.*, 110, B05504, doi:10.1029/2004JB003405.

Hardebeck, J. L. (2004), Stress triggering and earthquake probability estimates, *J. Geophys. Res.*, *109*, B04310, doi:10.1029/2003JB002437.

Heard, H. C. (1963), Effect of large changes in strain rate in the experimental deformation of Yule marble, *J. Geol.*, *71*, 162–195.

Hickman, J. B., E. N. Zhurina, and A. K. Kronenberg (1997), Deformation of talc and pyrophyllite: Disruption of van der Waals bonds and comparisons with calculated interlayer forces, *Eos Trans. AGU*, *78*, F724, Fall Meet. Suppl.

Hirata, T. (1987), Omori's power law aftershock sequences of microfracturing in rock fracture experiment, *J. Geophys. Res.*, *92*, 6215–6221.

Ibanez, W. D., and A. K. Kronenberg (1993), Experimental deformation of shale: Mechanical properties and microstructural indicators of mechanisms, *Int. J. Rock Mech. Min. Sci.*, *30*, 723–734.

Kato, N., K. Yamamoto, H. Yamamoto, and T. Hirasawa (1993), A stress-corrosion model for strain-rate dependence of the frictional strength of rocks, *Int J. Rock Mech. Min. Sci. Geomech. Abstr.*, *30*, 551–554.

Knopoff, L. (1972), Model of aftershock occurrence, in Flow and fracture of rocks, edited by H.C. Heard, I.Y. Borg, N.L. Carter, and C.B. Raleigh, Geophys. Monogr. Ser. 16, 259–263.

Kranz, R. L. (1980), The effects of confining pressure and stress difference on static fatigue of granite, *J. Geophys.*, 85.

Lawn, B. (1993), *Fracture of brittle solids*, 378pp, Cambridge Univ. Press, New York.

Linker, M. F., and J. H. Dieterich (1992), Effects of variable normal stress on rock friction: Observations and constitutive equations, *J. Geophys. Res.*, *97*, 4923–4940.

Lockner, D. A. (1998), A generalized law for brittle deformation of Westerly granite, *J. Geophys. Res.*, *103*, 5107–5123.

Marcellini, A. (1995), Arrhenius behavior of aftershock sequences, *J. Geophys. Res.*, *100*, 6463–6468.

Marcellini, A. (1997), Physical model of aftershock temporal behavior, *Tectonophysics*, *277*, 137–146.

Mares, V. M., and A. K. Kronenberg (1993), Experimental deformation of muscovite, *J. Struct. Geol.*, *15*, 1061–1075.

Marone, C., and B. Kilgore (1993), Scaling of the critical slip distance for seismic faulting with shear strain in fault zones, *Nature*, *362*, 618–621.

Meredith, P. G., and B. K. Atkinson (1982), High-temperature tensile crack propagation in quartz: Experimental results and application to time-dependent rupture, *Earthquake Predict. Res.*, *1*, 377–391.

Meredith, P. G., and B. K. Atkinson (1985), Fracture toughness and subcritical crack growth during high-temperature tensile deformation of Westerly granite and Black gabbro, *Phys. Earth Planet. Inter.*, *39*, 33–51.

Mogi, K. (1962), Study of elastic shocks caused by the fracture of heterogeneous materials and their relation to earthquake phenomenon, *Bull. Earthquake Res. Inst. Univ. Tokyo*, *40*, 1438.

Nakatani, M. (2001), Conceptual and physical clarification of rate and state friction: Frictional sliding as a thermally activated rheology, *J. Geophys. Res.*, *106*, 13,347–13,380.

Parsons, T. (2002), Omori law decay of triggered earthquakes: Large aftershocks outside the classical aftershock zone, *J. Geophys. Res.*, *107*, (B9), 2199, doi:10.1029/2001JB000646.

Parsons, T., S. Toda, R. S. Stein, A. Barka, and J. H. Dieterich (2000), Heightened odds of large earthquakes near Istanbul: An interaction-based probability calculation, *Science*, *288*, 661–665.

Reinen, L. A., J. D. Weeks, and T. E. Tullis (1994), The frictional behavior of lizardite and antigorite serpentinites: Experiments, constitutive models, and implications for natural faults, *Pure Appl. Geophys.*, *143*, 317–358.

Reuschle, T. (1990), Slow crack growth and aftershock sequences, *Geophys. Res. Lett.*, *17*, 1525–1528.

Rice, J. R., and A. L. Ruina (1983), Stability of steady frictional slipping, *J. Appl. Mech.*, *50*, 343–349.

Rice, J. R., N. Lapusta, and K. Ranjith (2001), Rate and state dependent friction an the stability of sliding between elastically deformable solids, *J. Mech. Phys. Solids*, *49*, 1865–1898.

Ruina, A. L. (1983), Slip instability and state variable friction laws, *J. Geophys. Res.*, *88*, 10,359–10,370.

Rutter, E. H. (1974), The influence of temperature, strain rate and interstitial water in the experimental deformation of calcite rocks, *Tectonophysics*, *22*, 311–334.

Saffer, D. M., and C. Marone (2003), Comparison of smectite and illite frictional properties: Application to the updip limit of the seismogenic zone along subduction megathrusts, *Earth Planet. Sci. Lett.*, *215*, 219–235.

Scholz, C. H. (1968a), Mechanism of creep in brittle rock, *J. Geophys. Res.*, *73*, 3295–3302.

Scholz, C. (1968b), Microfractures, aftershocks and seismicity, *Bull. Seismol. Soc. Am.*, *58*, 117–130.

Scholz, C. H. (1972), Static fatigue in quartz, *J. Geophys. Res.*, *77*, 2104–2114.

Scruggs, V. J. (1997), *Frictional constitutive properties and related microstructures of albite, muscovite, biotite and talc*, Ph. D. dissertation, Brown University, Providence, Rhode Island.

Scruggs, V. J., and T. E. Tullis (1998), Correlation between velocity dependence of friction and strain localization in large displacement experiments on feldspar, muscovite and biotite gouge, *Tectonophysics*, *295*, 15–40.

Stein, R. S., A. A. Barka, and J. H. Dieterich (1997), Progressive failure on the North Anatolian fault since 1939 by earthquake stress triggering, *Geophys. J. Int.*, *128*, 594–604.

Toda, S., and R. S. Stein (2002), Response of the San Andreas Fault to the 1983 Coalinga-Nuñez earthquakes: An application of interaction-based probabilities for Parkfield, *J. Geophys. Res.*, *107*, (B6), 2126, doi:10.1029/2001JB000172.

Toda, S., R. S. Stein, P. A. Reasenberg, and J. H. Dieterich (1998), Stress transferred by the 1995 Mw = 6/9 Kobe, Japan, shock: Effect on after-

shocks and future earthquake probabilities, *J. Geophys. Res.*, *103*, 24,543–24,564.
Tullis, T. E., and J. D. Weeks (1987), Micromechanics of frictional resistance of calcite, *Eos Trans. AGU*, *68*, 405.
Weeks, J. D., N. M. Beeler, and T. E. Tullis (1991), Glass is like a rock, *Eos Trans. AGU*, *72*.
Wiederhorn, S. M. (1978), Mechanisms of subcritical crack growth in glass, in *Fracture mechanics of ceramics*, vol. 4, 549–580, edited by R. C. Bradt, D. P. H. Hasselman, and F. F. Lange, Springer, New York.
Wiederhorn, S. M., and L. H. Bolz (1970), *J. Am. Ceram. Soc.*, *53*, 543–548.
Yamashita, Y., and L. Knopoff (1987), Models of aftershock occurrence, *Geophys. J. R. Astron. Soc.*, *91*, 13–26.

N. M. Beeler, US Geological Survey, 345 Middlefield Road, Menlo Park, CA 9405, USA. (nbeeler@usgs.gov)
A. K. Kronenberg, Texas A&M University, College Station, TX, USA.
L. A. Reinen, Pomona College, Pomona, CA, USA.
T. E. Tullis, Brown University, Providence, RI, USA.